Nicotinic acid adenine dinucleotide phosphate and cyclic ADP-ribose regulate TRPM2 channels in T lymphocytes

Andreas Beck,[1] Martin Kolisek,[1] Leigh Anne Bagley,[1] Andrea Fleig, and Reinhold Penner[2]

Laboratory of Cell and Molecular Signaling, Center for Biomedical Research at The Queen's Medical Center, and John A. Burns School of Medicine at the University of Hawaii, Honolulu, Hawaii, USA

To read the full text of this article, go to http://www.fasebj.org/cgi/doi/10.1096/fj.05-5538fje

SPECIFIC AIMS

TRPM2 is a Ca^{2+}-permeable non-selective cation channel that contains a C-terminal enzymatic domain with pyrophosphatase activity, which specifically binds ADP-ribose. Recent experiments have shown that cyclic ADP-ribose (cADPR) and hydrogen peroxide (H_2O_2) can facilitate ADPR-mediated activation of heterologously expressed TRPM2. This study aimed to determine whether two Ca^{2+}-mobilizing second messengers, specifically cADPR and nicotinic acid adenine dinucleotide phosphate (NAADP), could activate natively expressed TRPM2 channels in Jurkat T cells and to test the hypothesis whether these two agonists share a common binding site on TRPM2 that can regulate TRPM2 activity in synergy with ADPR.

PRINCIPAL FINDINGS

1. ADPR and cADPR activate native TRPM2 currents in Jurkat T cells.

Northern blotting has indicated that TRPM2 is expressed in a variety of tissues, and ADPR has been shown to produce currents (I_{ADPR}) in monocyte and T lymphocyte cell lines. To determine the characteristics of the I_{ADPR} current in Jurkat T lymphocytes, we performed whole-cell experiments using both ADPR and cADPR as channel activators. Our data revealed a maximum whole-cell current of ~500 pA at 1 mM internal ADPR (**Fig. 1*A***). A similar current size was reached at doses as low as 10 μM. cADPR induced maximum current sizes of around ~600 pA (Fig. 1*B*) but required slightly higher concentrations than ADPR and was effective at concentrations of 100 μM or higher. The linear current-voltage relationships of the currents produced by either agonist were indistinguishable from each other (Fig. 1*C*). The dose-response relationships derived from these whole-cell currents are shown in Fig. 1*D*. The half-maximal effective concentration (EC_{50}) for cADPR was found to be ~60 μM and that of ADPR was ~10 μM. These data indicate that the I_{ADPR} channel can be gated by both ADPR and cADPR in lymphocytes, although these cells are more sensitive to ADPR as a gating mechanism than to cADPR.

To establish that ADPR and cADPR can directly affect the I_{ADPR} channel in Jurkat cells, we applied either of these agonists to the internal side of cell-free inside-out membrane patches. Individual channel openings were observed using both ADPR and cADPR (Fig. 1*E*), although ADPR induced channel activity in only 11 out of 58 patches (19%), and cADPR was effective in 15 out of 111 patches (14%). The current-voltage relationships derived from these inside-out patches are shown in Fig. 1*F* and are virtually indistinguishable from each other. The single-channel conductance obtained by linear fits were 67 pS for ADPR and 69 pS for cADPR. These data indicate that the I_{ADPR} channel in Jurkat cells can be gated directly by either ADPR or cADPR in cell-free excised membrane patches.

2. ADPR- and cADPR-induced native TRPM2 currents in Jurkat cells have similar biophysical characteristics compared with heterologously expressed TRPM2 channels in HEK-293 cells.

The main difference we observed between heterologously expressed TRPM2 and the native I_{ADPR} in T cells was that the sensitivity of I_{ADPR} toward cADPR is significantly lower in T cells (EC_{50}=60 μM) compared with HEK-293 cells (EC_{50}=120 μM). In addition, the maximal current amplitudes obtained by cADPR in T cells are comparable with those achieved by ADPR, whereas our previous study found only a rather limited extent of cADPR-mediated activation. We considered that one possible reason for this discrepancy might reside in different intracellular pipette solutions used by the two studies, since the above T cell experiments were all performed using Cs-glutamate-based pipette solutions to minimize the lymphocyte's endogenous K^+ currents,

[1]These authors contributed equally to this work.

[2]Correspondence: Center for Biomedical Research, The Queen's Medical Center, 1301 Punchbowl St. UHT 8, Honolulu, HI 96813 USA. E-mail: rpenner@hawaii.edu.

doi: 10.1096/fj.05-5538fje

0892-6638/06/0020-0962 © FASEB

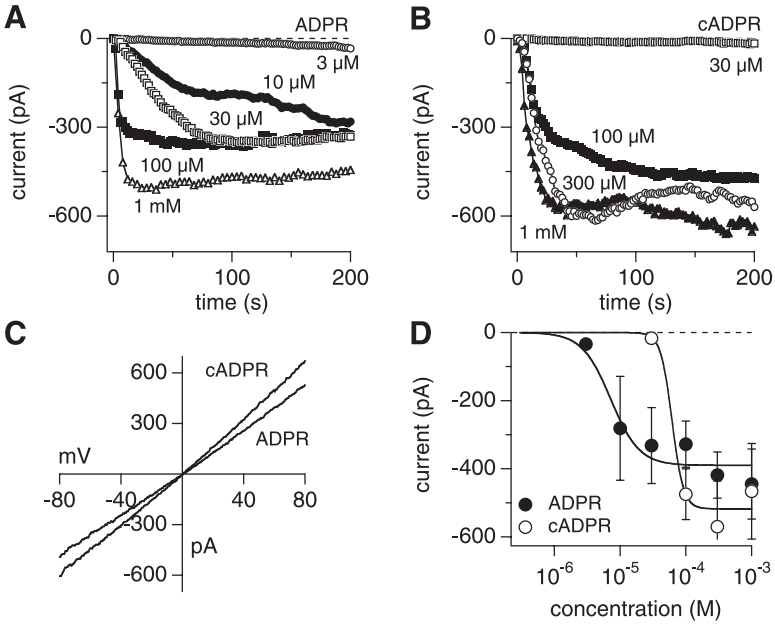

Figure 1. Native TRPM2 currents in Jurkat T cells. *A)* Average membrane currents recorded at −80 mV induced by perfusion of Jurkat cells with various concentrations of ADPR ranging from 3 μM to 1 mM (n=5–8) *(B)* Average membrane currents recorded at −80 mV induced with various concentrations of cADPR ranging from 30 μM to 1 mM (n=4–5). *C)* Representative current-voltage relationships derived from currents evoked by voltage ramps spanning −100 to + 100 mV. *D)* Dose-response relationships for I_{ADPR} in Jurkat cells evoked by ADPR (filled symbols) or cADPR (open symbols).

whereas our previous study on heterologously expressed TRPM2 in HEK- 293 cells was performed with K-glutamate-based solutions.

We therefore reassessed the ADPR and cADPR effects in both T cells and HEK-293 cells using K- and Cs-glutamate-based pipette solutions. Both ADPR and cADPR dose-dependently activated I_{ADPR} currents in K^+-based solutions. No significant change was found in the apparent sensitivity of TRPM2 to either ADPR or cADPR; the half-maximal effective concentrations for ADPR in the presence of Cs^+ and K^+ were 7 and 15 μM, respectively, and for cADPR they were 60 μM in both cases. The ADPR values are in close agreement to the EC_{50} values we determined in HEK-293 cells in Cs^+- and K^+-based solutions (15 and 12 μM, respectively). In both cell types, the maximal ADPR-induced current amplitudes were slightly smaller in the presence of Cs^+, suggesting that Cs^+ may actually reduce channel open probability. In contrast, we observed significant differences in the behavior of TRPM2 in both cell types when stimulating with cADPR. In T cells, TRPM2's sensitivity toward cADPR was unchanged, but current amplitudes were generally larger in the presence of Cs^+. In HEK-293 cells, cADPR was not very effective in K^+-based solutions, but Cs^+ shifted the EC_{50} by a factor of ~6 from 700 μM in the presence of K^+ to 120 μM in Cs^+-based solutions. In addition, the maximal cADPR-induced current amplitudes were larger in the presence of Cs^+. Thus, the overall sensitivity of the native channels in lymphocytes toward cADPR remains significantly higher than that of heterologously expressed TRPM2 in HEK-293 cells under either ionic condition.

3. NAADP activates TRPM2 in HEK-293 and Jurkat T cells.

More recently, a new Ca^{2+}-mobilizing messenger, nicotinic acid adenine dinucleotide phosphate (NAADP) has emerged. Like cADPR, NAADP can be produced via CD38 and like cADPR it appears to cause both Ca^{2+} release and Ca^{2+} influx, although no current consensus exists on whether NAADP targets the same receptor as cADPR. We considered the possibility that NAADP might affect TRPM2 channels and perfused HEK-293 cells expressing TRPM2 with various concentrations of

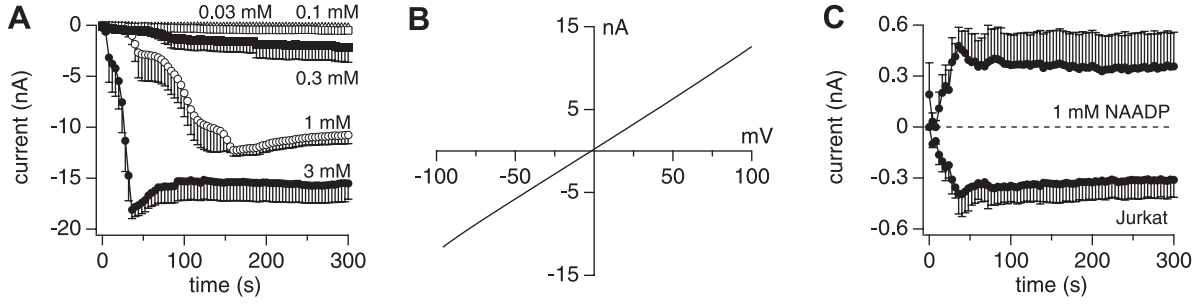

Figure 2. NAADP activates TRPM2 in HEK-293 and Jurkat T cells. *A)* Average membrane currents recorded at −80 mV induced by perfusion of TRPM2-expressing HEK-293 cells with various concentrations of NAADP ranging from 30 μM to 3 mM (n=4–7). *B)* Representative current-voltage relationship derived from currents evoked by voltage ramps spanning −100 to + 100 mV. *C)* Average membrane currents recorded at −80 and + 80 mV induced by perfusion of Jurkat T cells with 1 mM NAADP (n=5).

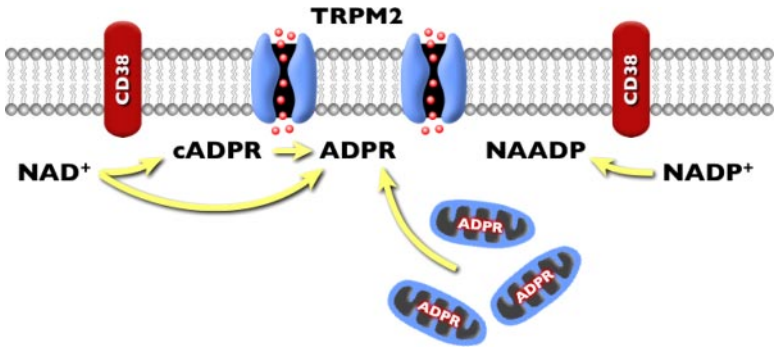

Figure 3. Proposed signaling mechanisms for TRPM2 Activation. Release or production of ADPR by mitochondria or the ectoenzyme CD38, respectively, act in synergy with cADPR, NAADP, or H_2O_2 to activate plasmalemmal TRPM2 ion channels.

this putative second messenger. NAADP indeed activated TRPM2 currents (**Fig. 2*A***) with a typical linear current-voltage relationship (Fig. 2*B*) and in a dose-dependent manner with an EC_{50} of 730 μM (Fig. 2*C*). We confirmed that NAADP could also activate I_{ADPR} in Jurkat T cells (Fig. 2*D*) and proceeded to characterize the NAADP mechanism in HEK-293 cells.

4. NAADP-induced TRPM2 currents are inhibited by both AMP and 8-Br-cADPR.

Since the efficacy of NAADP in activating TRPM2 was similar to that of cADPR, we reasoned that it might also synergize with ADPR at significantly lower concentrations. Indeed, when coperfusing cells with subthreshold concentrations of either nucleotide (nt) (100 μM NAADP+3 μM ADPR), we obtained full activation of TRPM2. Here, AMP fully suppressed current activation, confirming that NAADP sensitized TRPM2 gating by ADPR. This prompted us to test whether the NAADP mechanism was related to the one we demonstrated earlier for cADPR. We included the cADPR antagonist 8-Br-cADPR (100 μM), and this too inhibited the response to the co-applied NAADP and ADPR. This clearly suggests that NAADP is an integral part of the response and additionally suggests that its mechanism of action and binding site is the same as that for cADPR.

In light of the synergy between NAADP and ADPR, we asked whether the current activation seen with NAADP alone was entirely due to NAADP or contained an ADPR component that could arise from ADPR mobilization. The full TRPM2 activation by NAADP could be suppressed by both AMP and 8-Br-cADPR. This is consistent with the interpretation that NAADP, like cADPR, has some limited ability to gate TRPM2 directly even when the ADPR component is suppressed by AMP, whereas a direct antagonist like 8-Br-cADPR removes this effect as well.

CONCLUSIONS AND SIGNIFICANCE

Our results indicate that TRPM2, a Ca^{2+}-permeable nonselective cation channel natively expressed in lymphocytes, can be gated by ADPR and cADPR. We further conclude that NAADP acts in a very similar manner as cADPR in that it possesses a limited ability to gate TRPM2 directly, but strongly potentiates ADPR-mediated activation of the channel. An important observation in support of a synergy between cADPR and NAADP with ADPR is that intracellular administration of cADPR or NAADP apparently is accompanied by elevated levels of ADPR, which is further increased when using Cs^+-based intracellular solutions. At this point, we cannot ascribe this ADPR mobilization to a particular mechanism. The simplest explanation, that the nucleotides are metabolized to ADPR, faces the paradox that the best-characterized enzyme that could convert cADPR to ADPR, CD38, is an ectoenzyme and, therefore, not an obvious candidate to mediate this conversion. It is conceivable that other cytosolic enzymes yet to be characterized may be responsible for this phenomenon. Another explanation, that ADPR might be released from intracellular compartments, also cannot be readily explained, since the major store for ADPR is presumed to be mitochondrial and its possible release via cADPR or NAADP has not yet been documented.

An important question relates to the potency and physiological significance of cADPR- and NAADP-mediated activation of TRPM2, which occurs at relatively high concentrations of the second messengers; considerably higher than the nanomolar levels required to activate Ca^{2+} release. First, the nucleotide concentrations needed to activate TRPM2 in our patch-clamp experiments may not necessarily reflect the effective concentrations required to gate TRPM2 in intact cells. The differences we observed with K^+- and Cs^+-based pipette solutions attest to the fact that the intracellular environment does affect the sensitivity of TRPM2, and this is inevitably perturbed by whole-cell perfusion. Second, although recent evidence indicates that the receptor agonist cholecystokinin (CCK) can rapidly produce transient increases in NAADP and both CCK and acetylcholine can generate long-lasting increases in intracellular cADPR levels (27), there is no detailed knowledge about the global cytosolic or local subplasmalemmal concentrations that are achieved under specific physiological or pathological conditions. cADPR and NAADP may have a dual mode of action in that low concentrations can trigger Ca^{2+} release and higher concentrations additionally recruit TRPM2. Such a dual function of release activity and Ca^{2+} influx across the plasma membrane is not without precedent, as it has been demonstrated for the vanilloid receptor VR1. FJ

Nicotinic acid adenine dinucleotide phosphate and cyclic ADP-ribose regulate TRPM2 channels in T lymphocytes

Andreas Beck,[1] Martin Kolisek,[1] Leigh Anne Bagley,[1] Andrea Fleig, and Reinhold Penner[2]

Laboratory of Cell and Molecular Signaling, Center for Biomedical Research at The Queen's Medical Center, and John A. Burns School of Medicine at the University of Hawaii, Honolulu, Hawaii, USA

ABSTRACT **TRPM2 (previously designated TRPC7 or LTRPC2) is a Ca^{2+}-permeable nonselective cation channel that contains a C-terminal enzymatic domain with pyrophosphatase activity, which specifically binds ADP-ribose. Cyclic ADP-ribose (cADPR) and hydrogen peroxide (H_2O_2) can facilitate ADPR-mediated activation of heterologously expressed TRPM2. Here, we show that the two Ca^{2+}-mobilizing second messengers cyclic ADP-ribose (cADPR) and nicotinic acid adenine dinucleotide phosphate (NAADP) strongly activate natively expressed TRPM2 channels in Jurkat T cells. TRPM2 activation by both agonists can be partially suppressed by the ADPR antagonist adenosine monophosphate (AMP), which suggests that cADPR and NAADP lead to mobilization of endogenous ADPR presumably via metabolic conversion. The remaining channel activity is due to direct gating of TRPM2 by the two agonists and can be completely suppressed by 8-Br-cADPR, which suggests that cADPR and NAADP share a common binding site on TRPM2 that can regulate TRPM2 activity in synergy with ADPR. We conclude that cADPR and NAADP, in combination with ADPR, represent physiological co-activators of TRPM2 that contribute to Ca^{2+} influx in T lymphocytes and presumably other cell types that express this channel.—Beck, A., Kolisek, M., Bagley, L. A., Fleig, A., Penner, R. Nicotinic acid adenine dinucleotide phosphate and cyclic ADP-ribose regulate TRPM2 channels in T lymphocytes. *FASEB J.* 20, E47–E54 (2006)**

Key words: TRPM2 · cADPR · NAADP

The TRPM2 ion channel, previously named TRPC7 (1) or LTRPC2 (2, 3) and recently designated TRPM2 (4), has been shown to be a nonselective cation channel specifically gated by ADP-ribose (ADPR) (2, 3). Intracellular Ca^{2+} cannot activate TRPM2 by itself but appears to be an important modulator and cofactor of TRPM2, as elevated $[Ca^{2+}]_i$ can significantly increase the sensitivity of TRPM2 toward ADPR, enabling it to gate the channel at lower concentrations (2, 5). Early reports suggested that TRPM2 can also be gated by H_2O_2 (6) and high concentrations of NAD^+ (3, 6, 7), however, recent evidence suggests that the NAD^+ effect is likely due to contaminations of commercially available NAD^+ with ADPR and H_2O_2 has only very limited efficacy in activating TRPM2 directly (8). H_2O_2's primary mechanism of action appears to involve a facilitation of ADPR-mediated activation of TRPM2 (8), which is consistent with its apparent requirement for a functional ADPR binding site in the Nudix domain of the channel (9, 10). In close analogy to H_2O_2, cyclic ADP-ribose (cADPR) has recently been introduced as a further agonist for TRPM2 activation. It also has a limited ability to activate the channel directly but greatly potentiates ADPR-induced gating by shifting ADPR's half-maximal effective concentration from micromolar to nanomolar levels (8).

While TRPM2 is dominantly expressed in the brain, it is also detected in many other tissues, including bone marrow, spleen, heart, leukocytes, liver, and lung. Native TRPM2 currents have been recorded from the U937 monocyte cell line (2), neutrophils (7), microglia (11), and CRI-G1 insulinoma cells (12), where ADPR induces large cation currents (designated I_{ADPR}) that closely match those mediated by heterologously expressed TRPM2. Interestingly, many of the cell types in which TRPM2 is expressed (e.g., lymphocytes, neutrophils, pancreatic beta cells) have also been reported to utilize cADPR as a second messenger for Ca^{2+} signaling [for reviews see (13–19)]. Cyclic ADP-ribose is synthesized from its precursor NAD^+ by ADP-ribosyl cyclases (e.g., CD38) and has long been thought to function as an endogenous regulator of Ca^{2+}-induced Ca^{2+} release via ryanodine receptors. However, recent evidence has indicated that cADPR may also be involved in Ca^{2+} influx (20–22), and the discovery of its ability to target TRPM2 suggests that this Ca^{2+}-permeable channel may account for that effect (8). A further messenger that has emerged as Ca^{2+} release agonist is nicotinic acid adenine dinucleotide phosphate (NAADP) (18, 23–

[1] These authors contributed equally to this work.

[2] Correspondence: Center for Biomedical Research, The Queen's Medical Center, 1301 Punchbowl St. UHT 8, Honolulu, HI 96813. E-mail: rpenner@hawaii.edu.

doi: 10.1096/fj.05–5538fje

25), which can also be produced by CD38 from NADP. However, its molecular target has not yet been identified. Some studies suggest that NAADP, like cADPR, targets the ryanodine receptor, whereas others suggest an unknown release channel. Some evidence also points to a role of NAADP in Ca^{2+} influx (26). Both cADPR and NAADP have recently been found to be differentially produced following receptor stimulation and appear to serve a key role in initiating and maintaining cellular signaling in pancreatic acinar cells (27). In the present study, we have analyzed the effects of cADPR and NAADP on human TRPM2 channels expressed both heterologously in HEK-293 cells and natively in Jurkat T lymphocytes. We find that both messengers can activate these channels either directly and/or in synergy with ADPR and can, therefore, be regarded as genuine second messengers in support of Ca^{2+} influx.

MATERIALS AND METHODS

Cell culture

Tetracycline-inducible HEK-293 Flag-TRPM2-expressing cells (9, 10) were cultured at 37°C with 5% CO_2 in Dulbecco's modified Eagle's medium (DMEM) supplemented with 10% FBS, blasticidin (5 μg ml^{-1}; Invitrogen, Carlsbad, CA) and zeocin (0.4 mg ml^{-1}; Invitrogen). One to two days before the experiments, cells were resuspended in medium and plated on glass cover slips. TRPM2 expression was induced by 1 μg ml^{-1} tetracycline (Invitrogen) 15 h prior to experiments. Jurkat T cells were cultured at 37°C with 5% CO_2 in RPMI 1640 medium supplemented with 10% FBS.

Solutions

For patch-clamp experiments, cells were kept in standard Ringer's solution (in mM): 140 NaCl, 2.8 KCl, 1 $CaCl_2$, 2 $MgCl_2$, 10 glucose, 10 HEPES·NaOH (pH 7.2 adjusted with NaOH). Standard pipette-filling solutions contained (in mM): 140 Cs-glutamate, 8 NaCl, 1 $MgCl_2$, 10 Cs-BAPTA, 10 HEPES·CsOH (pH 7.2 adjusted with CsOH). In some experiments Cs-glutamate was replaced by K-glutamate, and Cs-BAPTA by K-BAPTA. In some other experiments, calcium was left unbuffered by leaving out any calcium chelator. Jurkat T cells were plated on coverslips coated with 25% polylysine 4–8 h before performing single-channel experiments using the inside-out configuration. Here, $[Ca^{2+}]_i$ and $[Ca^{2+}]_e$ were buffered to 200 nM with 10 mM BAPTA and 4.9 mM $CaCl_2$. All nucleotides and reagents were purchased from Sigma and dissolved in standard intracellular solution.

Electrophysiology

Patch-clamp experiments were performed in the whole-cell configuration at 21–25°C. All data were acquired with Pulse software controlling an EPC-9 amplifier (HEKA, Lambrecht, Germany) and analyzed using PulseFit (HEKA) and Igor Pro (Wavemetrics). Voltage ramps of 50 ms spanning the voltage range from –100 to + 100 mV were delivered from a holding potential of 0 mV at a rate of 0.5 Hz over a period of 200–500 s. When applicable, voltages were corrected for liquid junction potentials. Currents were filtered at 2.9 kHz and digitized at 100 μs intervals. Capacitive currents and series resistance were determined and corrected before each voltage ramp. For analysis, the very first current records before the activation of currents were digitally filtered at 2 kHz, pooled, and used for leak-subtraction of all subsequent records. The ramp current amplitudes at –80 mV (inward current) and +80 mV (outward current) were extracted from the leak-subtracted individual ramps and displayed as current development over time. Some individual ramps were displayed as representative current–voltage (I–V) relationships. Single-channel activity was recorded in the inside-out configuration and currents were filtered and sampled as above. Patches were pulled from Jurkat T cells and first exposed to the standard intracellular solution with $[Ca^{2+}]_i$ clamped to 200 nM. After 1 min of recordings in this solution, patches were exposed to the same solution supplemented with either 300 μM ADPR or 300 μM cADPR and monitored for channel activity. Single-channel data acquisition was performed using fixed voltage steps of 11 s duration given in 20 mV increments between –80 mV and +80 mV from a holding potential of 0 mV. For display purposes, data records were digitally filtered and down-sampled to 100 Hz.

RESULTS

Northern blotting has indicated that TRPM2 is expressed in a variety of tissues and cell types, including immunocytes (1–3). Further, ADPR has been shown to produce I_{ADPR} in monocyte and T lymphocyte cell lines (2, 3). To determine the characteristics of the I_{ADPR} in Jurkat T lymphocytes, we performed whole-cell experiments using both ADPR and cADPR as channel activators. These experiments were performed under relatively physiological conditions in which $[Ca^{2+}]_i$ was left unbuffered and allowed to vary freely by leaving out any extrinsic calcium chelators. Our data revealed a maximum whole-cell inward current of ~500 pA at 1 mM internal ADPR (**Fig. 1*A***). A similar current size was reached at doses as low as 10 μM, with longer times to reach maximum current as concentrations decreased. Similarly, cADPR induced maximum inward current sizes of around ~600 pA (Fig. 1*B*), but required slightly higher concentrations than ADPR and was effective at concentrations of 100 μM or higher. The linear current-voltage relationships of the currents produced by either agonist were indistinguishable from each other (Fig. 1*C*). The dose-response relationships derived from these whole-cell currents are shown in Fig. 1*D*. The half-maximal effective concentration (EC_{50}) for cADPR was found to be ~60 μM and that of ADPR was ~10 μM. These data indicate that the I_{ADPR} channel can be gated by both ADPR and cADPR in lymphocytes, although under these experimental conditions these cells are more sensitive to ADPR as a gating mechanism than to cADPR.

To establish whether ADPR and cADPR could directly affect the I_{ADPR} channel in Jurkat cells, we applied either of these agonists to the internal side of cell-free inside-out membrane patches. Individual channel openings were observed using both ADPR and cADPR (Fig. 1*E*), though ADPR induced channel activity in only 11 out of 58 patches (19%), and cADPR was effective in 15 out of 111 patches (14%). However,

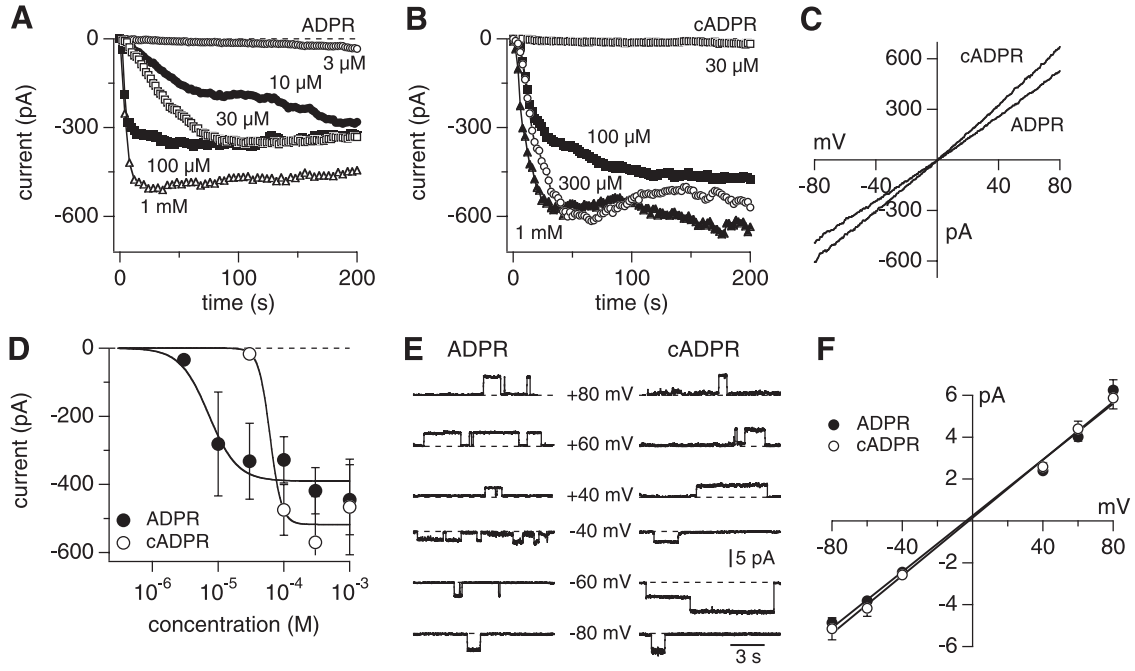

Figure 1. ADPR and cADPR activate native TRPM2 currents in Jurkat T cells. All experiments were performed using Cs-glutamate-based pipette solutions. *A)* Average membrane currents recorded at −80 mV induced by perfusion of Jurkat cells with various concentrations of ADPR ranging from 3 μM to 1 mM (n=5–8) (300 μM data not shown as it almost exactly overlaps the 1 mM data set). Note the slower time to full activation at lower concentrations. *B)* Average membrane currents recorded at −80 mV induced by perfusion of Jurkat cells with various concentrations of cADPR ranging from 30 μM to 1 mM (n=4–5). *C)* Representative current-voltage relationships derived from currents evoked by voltage ramps spanning −100 to +100 mV in two typical cells that responded to ADPR and cADPR. *D)* Dose-response relationships for I_{ADPR} in Jurkat cells. Cells were perfused with defined concentrations of ADPR (filled symbols) and cADPR (open symbols). External calcium concentration was 1 mM and $[Ca^{2+}]_i$ was left unbuffered. Data points represent the average current amplitudes ± SEM (n=4–8) at −80 mV measured at 200 s after break-in. The averaged data points were fitted with a dose-response curve yielding an apparent EC_{50} of 7 and 60 μM for ADPR and cADPR, respectively. Hill coefficients were 2 for ADPR and 5 for cADPR. *E)* Single-channel activity at various voltage levels in inside-out patches excised from Jurkat cells and exposed to 300 μM ADPR (left column, samples are from 4 different patches) or 300 μM cADPR (right column, samples are from 5 different patches). The inside solutions containing ADPR or cADPR were Cs-glutamate-based and the pipette solutions (facing the outside of the patch) were NaCl-based, both buffered to 200 nM free $[Ca^{2+}]$. *F)* Current-voltage relationships of single channels from Jurkat cells. Closed symbols represent ADPR and open symbols represent cADPR. Each data point represents the average amplitude of several events ± SEM from different patches (n=4–5) plotted vs. test voltage. A linear fit to the data points yielded a single-channel conductance of 67 pS for ADPR and 69 pS for cADPR.

patches that exhibited ADPR/cADPR-responsive channels often contained several ion channels, indicating that native channels in lymphocytes may be clustered. The current-voltage relationships derived from these inside-out patches are shown in Fig. 1*F* and are virtually indistinguishable. The single-channel conductance, obtained by linear fits, were 67 pS for ADPR and 69 pS for cADPR. These data indicate that the I_{ADPR} channel in Jurkat cells can be gated directly by either ADPR or cADPR in cell-free excised membrane patches.

The above results confirm our previous observation that cADPR can indeed regulate TRPM2 activity (8). The main difference we observed between heterologously expressed TRPM2 and the native I_{ADPR} in T cells was that the sensitivity of I_{ADPR} toward cADPR appears to be significantly lower in T cells (EC_{50} = 60 μM) compared with HEK-293 cells (EC_{50} = 120 μM). In addition, the maximal current amplitudes obtained by cADPR in T cells are comparable to those achieved by ADPR, whereas our previous study found only a rather limited extent of cADPR-mediated activation, typically amounting to less than 5% of the maximal current induced by ADPR (8). We considered that one possible reason for this discrepancy might reside in different intracellular pipette solutions used by the two studies, since the above T cell experiments were all performed using Cs-glutamate-based pipette solutions to minimize the lymphocyte's endogenous K^+ currents, whereas our previous study on heterologously expressed TRPM2 in HEK-293 cells was performed with K-glutamate-based solutions.

To determine whether Cs^+ might account for the enhanced cADPR responses in T cells, we reassessed the ADPR and cADPR effects in both T cells and HEK-293 cells using K- and Cs-glutamate-based pipette solutions. As illustrated in **Figs. 2*A*** and ***B***, both ADPR and cADPR dose-dependently activated I_{ADPR} currents in K^+-based solutions. We found no significant change in the apparent sensitivity of TRPM2 to either ADPR (Fig. 2*C*) or cADPR (Fig. 2*D*); the half-maximal effective concentrations for ADPR in the presence of Cs^+ and K^+ were 7 and 15 μM, respectively, and for cADPR

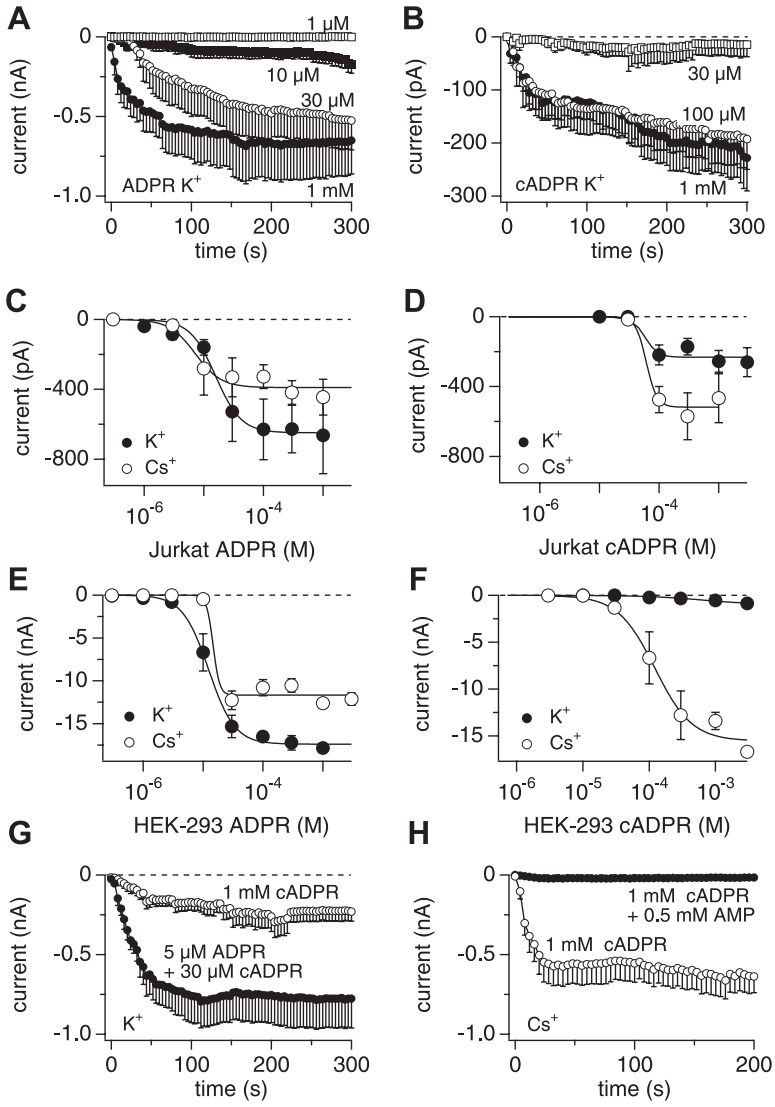

Figure 2. Comparison of ADPR- and cADPR-induced TRPM2 currents in Jurkat and HEK-293 cells. All experiments were performed using either Cs-glutamate- or K-glutamate-based pipette solutions. *A)* Average membrane currents (–SEM) over time recorded at –80 mV induced by perfusion of Jurkat cells with various concentrations of ADPR ranging from 1 μM to 1 mM (n=5–9) in K-glutamate-based solutions. *B)* Average membrane currents (–SEM) recorded at –80 mV induced by perfusion of Jurkat cells with various concentrations of cADPR ranging from 30 μM to 1 mM (n=4–27). *C)* Dose-response relationships for cation currents in Jurkat cells perfused with defined concentrations of ADPR in K^+- (filled symbols) and Cs^+-based solutions (open symbols). External calcium concentration was 1 mM and $[Ca^{2+}]_i$ was left unbuffered. Data points represent the average current amplitudes ± SEM (n=5–9) measured at 300 s after break-in at –80 mV. The averaged data points were fitted with a dose-response curve yielding an apparent EC_{50} of 15 μM in Cs^+ and 7 μM in K^+, respectively. Hill coefficient was 2 in each case. *D)* Dose-response relationships for cation currents in Jurkat cells perfused with defined concentrations of cADPR in K^+- (filled symbols) and Cs^+-based solutions (open symbols). External calcium concentration was 1 mM and $[Ca^{2+}]_i$ was left unbuffered. Data points represent the average current amplitudes ± SEM (n=4–27) measured at 300 s after break-in at –80 mV. The averaged data points were fitted with a dose-response curve yielding an apparent EC_{50} of 60 μM for both Cs^+ and in K^+ with Hill coefficients of 5. *E)* Dose-response relationships for TRPM2 currents in HEK-293 cells perfused with defined concentrations of ADPR in K^+- (filled symbols) and Cs^+-based solutions (open symbols). External calcium concentration was 1 mM and $[Ca^{2+}]_i$ was left unbuffered. Data points represent the average peak current amplitudes ± SEM (n=3–13) measured at –80 mV. The averaged data points were fitted with a dose-response curve yielding an apparent EC_{50} of 15 μM in Cs^+ and 12 μM in K^+ (K^+ data reproduced from Kolisek et al. *Mol. Cell* 18 (2005) Fig 1*E*, with permission), respectively. Hill coefficients were 5 and 1, respectively. *F)* Dose-response relationships for TRPM2 currents in HEK-293 cells perfused with defined concentrations of cADPR in K^+- (filled symbols, the data point for 10 μM is masked by the open symbols) and Cs^+-based solutions (open symbols). External calcium concentration was 1 mM and $[Ca^{2+}]_i$ was left unbuffered. Data points represent the average current amplitudes ± SEM (n=5–6) measured at 300 s after break-in at –80 mV. The averaged data points were fitted with a dose-response curve yielding an apparent EC_{50} of 120 μM in Cs^+ and 700 μM in K^+, respectively. Hill coefficients were 1.5 and 1, respectively. *G)* Average membrane currents (–SEM) over time recorded at –80 mV induced by perfusion of Jurkat cells with 1 mM cADPR alone (open symbols; n=6) or a combination of 30 μM cADPR plus 5 μM ADPR (filled symbols; n=5). In both cases, a K^+-based solution was used. *H)* Average membrane currents (–SEM) recorded at –80 mV induced by perfusion of Jurkat cells with 1 mM cADPR in the absence (open symbols; n=5) or presence of 500 μM AMP (filled symbols; n=3). In both cases, a Cs^+-based solution was used.

they were 60 μM in both cases. The ADPR values are in close agreement to the EC_{50} values we determined in HEK-293 cells in Cs^+ and K^+-based solutions 15 and 12 μM, respectively (Fig. 2*E*). In both cell types, the maximal ADPR-induced current amplitudes were slightly smaller in the presence of Cs^+, suggesting that Cs^+ may actually reduce channel open probability. In contrast, we observed significant differences in the behavior of TRPM2 in both cell types when stimulating with cADPR. In T cells (Fig. 2*D*), TRPM2's sensitivity toward cADPR was unchanged, but current amplitudes were generally larger in the presence of Cs^+. In HEK-293 cells (Fig. 2*F*), as previously reported, cADPR was not very effective in K^+-based solutions, but Cs^+ shifted the EC_{50} by a factor of ~6 from 700 μM in the presence of K^+ to 120 μM in Cs^+-based solutions. In addition, the maximal cADPR-induced current amplitudes were larger in the presence of Cs^+, reaching levels normally only obtained with ADPR. Thus, the overall sensitivity of the native channels in lymphocytes toward cADPR remains significantly higher than that of heterologously expressed TRPM2 in HEK-293 cells under either ionic condition.

The above results indicate that Cs^+ ions can enhance

cADPR-mediated gating of TRPM2 compared with the more physiological cation K^+. In HEK-293 cells, it causes a shift in the apparent EC_{50} to lower concentrations and in both HEK-293 cells and T cells it enhances maximal current amplitudes. It seems unlikely that this facilitatory effect is due to a direct action on the channel's functional properties, since Cs^+ does not significantly affect EC_{50} values of ADPR-mediated currents and current amplitudes are actually reduced rather than enhanced. It is also unlikely that Cs^+ simply enhances cADPR's affinity for TRPM2, since there is no shift in the apparent EC_{50} for cADPR in T cells. This finding suggests that the differences observed in T cells and HEK-293 cells are likely based on the cellular environment the channels are embedded in. For example, Cs^+ might mobilize endogenous ADPR either by releasing it from internal compartments such as mitochondria or by enhancing the enzymatic production of ADPR from cADPR, which would then synergize with cADPR to produce enhanced TRPM2 activity. Since T cells express native nucleotide-regulated TRPM2 channels, it seems plausible that T cells might be equipped with a more efficient enzymatic machinery for metabolizing adenine dinucleotides compared with HEK-293 cells. This would also explain why T cell currents are already enhanced relative to HEK-293 cells even in K^+-based solutions.

To test the above hypothesis, we performed two types of experiments. We first confirmed that the synergy between cADPR and ADPR previously observed in heterologously expressed TRPM2 also applies to native I_{ADPR} by co-applying subthreshold concentrations of cADPR (30 μM) and ADPR (5 μM) using K^+-based pipette solutions in T cells. At these subthreshold concentrations, neither of the agonists applied alone would activate I_{ADPR}. However, their combined presence resulted in full activation of I_{ADPR} currents that were significantly larger than those obtained by 1 mM cADPR alone (Fig. 2*G*). In a second set of experiments, we determined whether the full activation of I_{ADPR} induced by a high concentration of cADPR alone (1 mM) in a Cs^+-based pipette solution was in part due to endogenous ADPR mobilization. We took advantage of AMP, which we have previously shown to inhibit ADPR—but not cADPR—mediated gating of TRPM2. Also, we reasoned that if ADPR contributed to the cADPR response, AMP should prevent the full activation. As illustrated in Fig. 2*H*, AMP indeed prevented the full activation of cADPR-induced I_{ADPR}, leaving only a small current that presumably reflects the direct gating of TRPM2 by cADPR. This finding suggests that T cells indeed produce significant ADPR levels from cADPR and the combined presence of both agonists fully activates TRPM2 channels. In HEK-293 cells, the mobilization of ADPR in K^+-based solutions may not be sufficient to trigger full activation, whereas Cs^+ might just be able to mobilize enough ADPR to cause the synergistic activation.

Our finding that cADPR activates I_{ADPR} currents has important implications for cADPR function. Most studies demonstrate that cADPR acts through the ryanodine receptor to release Ca^{2+} from internal stores. There is, however, some indication that cADPR may also play a role in calcium entry in some cell types. The first report to suggest that cADPR may gate a cation channel came from ascidian oocytes, where ADPR was identified as the primary gating mechanism for an ion channel that triggers the fertilization response and cADPR was also found to be effective (28). The properties of that ion channel, however, are quite different from of TRPM2. More directly relevant to the context of the current study is the fact that cADPR was found to induce Ca^{2+} influx in T cells by producing spikes of $[Ca^{2+}]_i$ over long time periods that were dependent on the presence of extracellular Ca^{2+} (20). Since TRPM2 was unknown at that time, this calcium entry was not attributed to calcium influx through any particular ion channel. cADPR also appears to be required for sustained extracellular Ca^{2+} influx in neutrophils that have been stimulated by the bacterial chemoattractant, formyl-methionyl-leucyl-phenylalanine (fMLP), since the sustained Ca^{2+} influx phase of neutrophils derived from transgenic mice that lack the ADP-ribosyl cyclase CD38 is greatly reduced (22). The data presented here show that cADPR may in fact directly gate a plasma membrane ion channel in support of Ca^{2+} influx and may underlie the cADPR-mediated Ca^{2+} influx observed in these cell types.

More recently, a new Ca^{2+}-mobilizing messenger, nicotinic acid adenine dinucleotide phosphate (NAADP), has emerged (18, 23–25). Like cADPR, NAADP can be produced via CD38 and like cADPR it appears to cause both Ca^{2+} release and Ca^{2+} influx, although there is currently no consensus on whether NAADP targets the same receptor as cADPR. We considered the possibility that NAADP might affect TRPM2 channels and perfused HEK-293 cells expressing TRPM2 with various concentrations of this putative second messenger. NAADP indeed activated TRPM2 currents (**Fig. 3*A***) with a typical linear current-voltage relationship (Fig. 3*B*) and in a dose-dependent manner with an EC_{50} for of 730 μM (Fig. 3*C*). We confirmed that NAADP could also activate I_{ADPR} in Jurkat T cells (Fig. 3*D*) and proceeded to characterize the NAADP mechanism in HEK-293 cells.

Since the efficacy of NAADP in activating TRPM2 was similar to that of cADPR, we reasoned that it might also synergize with ADPR at significantly lower concentrations. Indeed, when co-perfusing cells with subthreshold concentrations of either nt (100 μM NAADP+3 μM ADPR), we obtained full activation of TRPM2 (**Fig. 4*A***). Under these experimental conditions, AMP fully suppressed current activation, confirming that NAADP sensitized TRPM2 gating by ADPR. This prompted us to test whether the NAADP mechanism was related to the one we demonstrated earlier for cADPR. We included the cADPR antagonist 8-Br-cADPR (100 μM), and this too inhibited the response to the co-applied NAADP and ADPR (Fig. 4*A*). This clearly suggests that NAADP is an integral part of the response and additionally

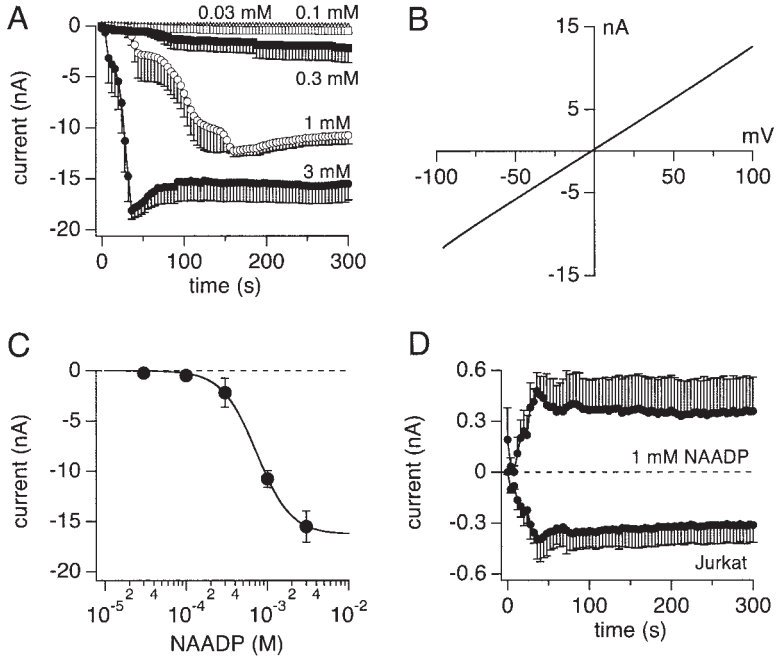

Figure 3. NAADP activates TRPM2 in HEK-293 and Jurkat T cells. All experiments were performed using K-glutamate-based pipette solutions. *A)* Average membrane currents (–SEM) recorded at –80 mV induced by perfusion of TRPM2-expressing HEK-293 cells with various concentrations of NAADP ranging from 30 μM to 3 mM (n=4–7). *B)* Representative current-voltage relationship derived from currents evoked by voltage ramps spanning –100 to + 100 mV. *C)* Dose-response relationship for NAADP-induced currents in HEK-293 cells. Cells were perfused with defined concentrations of NAADP. External calcium concentration was 1 mM and $[Ca^{2+}]_i$ was left unbuffered. Data points represent the average current amplitudes (–SEM; n=4–7) measured at peak amplitude after break-in at –80 mV. The averaged data points were fitted with a dose-response curve yielding an apparent EC_{50} of 730 μM with a Hill coefficient of 2. *D)* Average inward current (–SEM) recorded at –80 mV and outward current (–SEM) recorded at + 80 mV induced by perfusion of Jurkat T cells with 1 mM NAADP (n=5).

suggests that its mechanism of action and binding site is the same as that for cADPR.

In light of the synergy between NAADP and ADPR, we asked whether the current activation seen with NAADP alone was entirely due to NAADP or contained an ADPR component that could arise from ADPR mobilization. Fig. 4*B* demonstrates that the full TRPM2 activation by NAADP could be suppressed by both AMP and 8-Br-cADPR and Fig. 4*C* illustrates the remaining currents at higher resolution. It can be seen that AMP leaves a small remaining current, whereas 8-Br-cADPR causes a complete block of the current. This finding is consistent with the interpretation that NAADP, like cADPR, has some limited ability to gate TRPM2 directly even when the ADPR component is suppressed by AMP, whereas a direct antagonist like 8-Br-cADPR removes this effect as well.

DISCUSSION

Our results indicate that TRPM2, a Ca^{2+}-permeable nonselective cation channel natively expressed in lymphocytes, can be gated by ADPR and cADPR. This gating can be observed in both whole-cell experiments, as well as in cell-free inside-out experiments indicating that both ADPR and cADPR act directly on the TRPM2 channel. We further demonstrate that NAADP acts in a very similar manner as cADPR in that it possesses a limited ability to gate TRPM2 directly, but strongly potentiates ADPR-mediated activation of the channel. An important observation in support of a synergy between cADPR and NAADP with ADPR is that intracellular administration of cADPR or NAADP apparently is accompanied by elevated levels of ADPR, which is further increased when using Cs^{+}-based intracellular

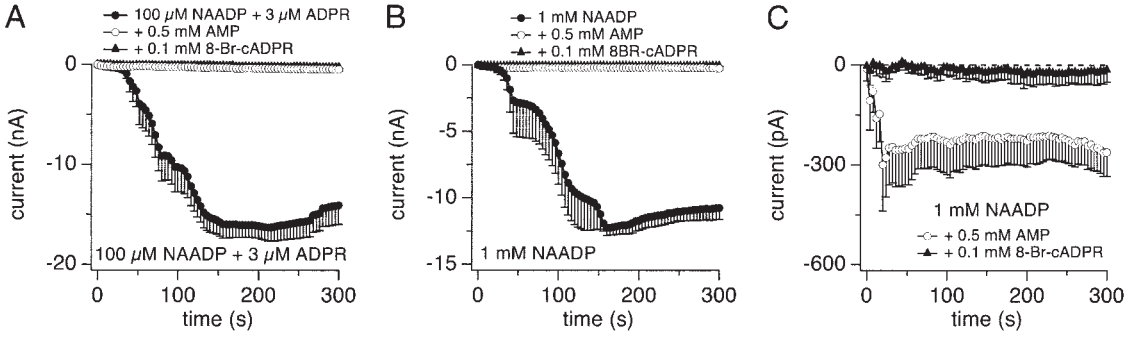

Figure 4. NAADP-induced TRPM2 currents are inhibited by both AMP and 8-Br-cADPR. *A)* Average membrane currents (–SEM) recorded at –80 mV induced by perfusion of TRPM2-expressing HEK-293 cells with a combination of 100 μM NAAPD plus 3 μM ADPR in control cells (filled circles; n=11) and the additional presence of either 500 μM AMP (open circles; n=6) or 100 μM 8-Br-cADPR (filled triangles, masked by the AMP data; n=5). *B)* Average membrane currents (–SEM) recorded at –80 mV induced by perfusion of TRPM2-expressing HEK-293 cells with 1 mM NAAPD in control cells (filled circles; n=5) and the additional presence of either 500 μM AMP (open circles; n=5) or 100 μM 8-Br-cADPR (filled triangles, masked by the AMP data; n=5). *C)* Expanded plot of the currents inhibited by AMP (open circles) and 8-Br-cADPR (filled triangles) shown in *(B)* to illustrate the higher blocking efficacy of 8-Br-cADPR compared with AMP.

solutions. At this point, we cannot ascribe this ADPR mobilization to a particular mechanism. The simplest explanation, that the nucleotides are metabolized to ADPR, faces the paradox that the best-characterized enzyme that could convert cADPR to ADPR, CD38, is an ectoenzyme and, therefore, not an obvious candidate to mediate this conversion. It is conceivable that other cytosolic enzymes yet to be characterized may be responsible for this phenomenon. Another explanation, that ADPR might be released from intracellular compartments, also cannot be readily explained, since the major store for ADPR is presumed to be mitochondrial and its possible release via cADPR or NAADP has not yet been documented.

Our findings raise a number of important questions regarding the specificity and the physiological function of cADPR and NAADP. We consider the effects of these nucleotides to be specific, since other nucleotides fail to activate TRPM2 even at high concentrations (2). Specificity is also evident from the fact that the cADPR antagonist 8-Br-cADPR completely blocks both cADPR- and NAADP-mediated gating of TRPM2, which suggests that both agonists access the same binding site on TRPM2. This binding site is clearly distinct from that of ADPR, since 8-Br-cADPR does not affect the activation by ADPR. Conversely, the direct activation of TRPM2 by cADPR and NAADP, albeit limited, cannot be suppressed by the specific ADPR antagonist AMP.

Another important question relates to the potency and physiological significance of cADPR- and NAADP-mediated activation of TRPM2, which occurs at relatively high concentrations of the second messengers; considerably higher than the nanomolar levels required to activate Ca^{2+} release. First, the nucleotide concentrations needed to activate TRPM2 in our patch-clamp experiments may not necessarily reflect the effective concentrations required to gate TRPM2 in intact cells. The differences we observed with K^+- and Cs^+-based pipette solutions attest to the fact that the intracellular environment does affect the sensitivity of TRPM2 and this is inevitably perturbed by whole-cell perfusion. Second, although recent evidence obtained in pancreatic acinar cells indicates that the receptor agonist cholecystokinin (CCK) can rapidly produce transient increases in NAADP and both CCK and acetylcholine can generate long-lasting increases in intracellular cADPR levels (27), there is no detailed knowledge about the global cytosolic or local subplasmalemmal concentrations that are achieved under specific physiological conditions. So far, only one study has assessed NAADP concentrations and arrived at low micromolar levels in sea urchin eggs (29). Higher levels of NAADP might occur under some pathological conditions caused, e.g., by enhanced activity of enzymes that generate NADP or by reduced activity of enzymes that metabolize it. It is conceivable that cADPR and NAADP can have a dual mode of action in that low concentrations can trigger Ca^{2+} release and higher concentrations additionally recruit TRPM2. Although highly speculative, it is even possible that TRPM2 might be expressed in intracellular compartments and also serve as a release channel, where it may have a different sensitivity toward cADPR/NAADP, possibly due to being exposed to an intraorganellar acidic environment. Such a dual function of release activity and Ca^{2+} influx across the plasma membrane is not without precedent, as it has been demonstrated for the vanilloid receptor VR1 (30). Our present demonstration that cADPR and NAADP share a common target in activating TRPM2 might also indicate a common target that mediates their Ca^{2+} release activity regardless of whether the release activity is or is not mediated by TRPM2. Our present knowledge only allows us to conclude that if we accept cADPR and NAADP as genuine and relevant activators of TRPM2 either in the plasma membrane or in Ca^{2+} stores, then we must assume that these messengers are in fact produced at the relevant concentrations needed to do so. Finally, cADPR and NAADP may not represent primary or singular activators of TRPM2, but rather synergistic co-activators. It is likely that these messengers are produced along with additional factors that could significantly shift the sensitivity of TRPM2 toward them. One such factor is $[Ca^{2+}]_i$, and there could be other signaling pathways that synergize with $[Ca^{2+}]_i$ and ADPR/cADPR/NAADP to enable TRPM2 gating at concentrations that are achieved physiologically. FJ

We thank Mahealani K. Monteilh-Zoller and Ka'ohimanu L. Dang for expert technical assistance. This work was supported in part by the following grants from the National Institutes of Health: R01-NS40927, R01-AI50200 and R01-GM 063954 to R.P. and R01-GM 65360 to A.F.

REFERENCES

1. Nagamine, K., Kudoh, J., Minoshima, S., Kawasaki, K., Asakawa, S., Ito, F., and Shimizu, N. (1998) Molecular cloning of a novel putative Ca^{2+} channel protein (TRPC7) highly expressed in brain. *Genomics* **54,** 124–131
2. Perraud, A. L., Fleig, A., Dunn, C. A., Bagley, L. A., Launay, P., Schmitz, C., Stokes, A. J., Zhu, Q., Bessman, M. J., Penner, R., Kinet, J. P., and Scharenberg, A. M. (2001) ADP-ribose gating of the calcium-permeable LTRPC2 channel revealed by Nudix motif homology. *Nature* **411,** 595–599
3. Sano, Y., Inamura, K., Miyake, A., Mochizuki, S., Yokoi, H., Matsushime, H., and Furuichi, K. (2001) Immunocyte Ca^{2+} influx system mediated by LTRPC2. *Science* **293,** 1327–1330
4. Montell, C., Birnbaumer, L., Flockerzi, V., Bindels, R. J., Bruford, E. A., Caterina, M. J., Clapham, D. E., Harteneck, C., Heller, S., Julius, D., Kojima, I., Mori, Y., Penner, R., Prawitt, D., Scharenberg, A. M., Schultz, G., Shimizu, N., and Zhu, M. X. (2002) A unified nomenclature for the superfamily of TRP cation channels. *Mol. Cell* **9,** 229–231
5. McHugh, D., Flemming, R., Xu, S. Z., Perraud, A. L., and Beech, D. J. (2003) Critical intracellular Ca^{2+} dependence of transient receptor potential melastatin 2 (TRPM2) cation channel activation. *J. Biol. Chem.* **278,** 11002–11006
6. Hara, Y., Wakamori, M., Ishii, M., Maeno, E., Nishida, M., Yoshida, T., Yamada, H., Shimizu, S., Mori, E., Kudoh, J., Shimizu, N., Kurose, H., Okada, Y., Imoto, K., and Mori, Y. (2002) LTRPC2 Ca^{2+}-permeable channel activated by changes in redox status confers susceptibility to cell death. *Mol. Cell* **9,** 163–173
7. Heiner, I., Eisfeld, J., and Luckhoff, A. (2003) Role and regulation of TRP channels in neutrophil granulocytes. *Cell Calcium* **33,** 533–540

8. Kolisek, M., Beck, A., Fleig, A., and Penner, R. (2005) Cyclic ADP-ribose and hydrogen peroxide synergize with ADP-ribose in the activation of TRPM2 channels. *Mol. Cell* **18,** 61–69
9. Kuhn, F. J., and Luckhoff, A. (2004) Sites of the NUDT9-H domain critical for ADP-ribose activation of the cation channel TRPM2. *J. Biol. Chem.* **279,** 46431–46437
10. Perraud, A. L., Takanishi, C. L., Shen, B., Kang, S., Smith, M. K., Schmitz, C., Knowles, H. M., Ferraris, D., Li, W., Zhang, J., Stoddard, B. L., and Scharenberg, A. M. (2005) Accumulation of free ADP-ribose from mitochondria mediates oxidative stress-induced gating of TRPM2 cation channels. *J. Biol. Chem.* **280,** 6138–6148
11. Kraft, R., Grimm, C., Grosse, K., Hoffmann, A., Sauerbruch, S., Kettenmann, H., Schultz, G., and Harteneck, C. (2004) Hydrogen peroxide and ADP-ribose induce TRPM2-mediated calcium influx and cation currents in microglia. *Am. J. Physiol. Cell Physiol.* **286,** C129–137
12. Inamura, K., Sano, Y., Mochizuki, S., Yokoi, H., Miyake, A., Nozawa, K., Kitada, C., Matsushime, H., and Furuichi, K. (2003) Response to ADP-ribose by activation of TRPM2 in the CRI-G1 insulinoma cell line. *J. Membr. Biol.* **191,** 201–207
13. Galione, A., and Churchill, G. C. (2000) Cyclic ADP ribose as a calcium-mobilizing messenger. *Sci. STKE.* 2000, PE1
14. Galione, A., and Churchill, G. C. (2002) Interactions between calcium release pathways: multiple messengers and multiple stores. *Cell Calcium* **32,** 343–354
15. Lee, H. C., Munshi, C., and Graeff, R. (1999) Structures and activities of cyclic ADP-ribose, NAADP and their metabolic enzymes. *Mol. Cell Biochem.* **193,** 89–98
16. Lee, H. C. (2000) Multiple calcium stores: separate but interacting. *Sci. STKE* 2000, PE1
17. Dousa, T. P., Chini, E. N., and Beers, K. W. (1996) Adenine nucleotide diphosphates: emerging second messengers acting via intracellular Ca^{2+} release. *Am. J. Physiol.* **271,** C1007–1024
18. Guse, A. H. (2002) Cyclic ADP-ribose (cADPR) and nicotinic acid adenine dinucleotide phosphate (NAADP): novel regulators of Ca^{2+}-signaling and cell function. *Curr. Mol. Med.* **2,** 273–282
19. Lund, F. E., Cockayne, D. A., Randall, T. D., Solvason, N., Schuber, F., and Howard, M. C. (1998) CD38: a new paradigm in lymphocyte activation and signal transduction. *Immunol. Rev.* **161,** 79–93
20. Guse, A. H., Berg, I., da Silva, C. P., Potter, B. V., and Mayr, G. W. (1997) Ca^{2+} entry induced by cyclic ADP-ribose in intact T-lymphocytes. *J. Biol. Chem.* **272,** 8546–8550
21. Guse, A. H., da Silva, C. P., Berg, I., Skapenko, A. L., Weber, K., Heyer, P., Hohenegger, M., Ashamu, G. A., Schulze-Koops, H., Potter, B. V., and Mayr, G. W. (1999) Regulation of calcium signalling in T lymphocytes by the second messenger cyclic ADP-ribose. *Nature* **398,** 70–73
22. Partida-Sanchez, S., Cockayne, D. A., Monard, S., Jacobson, E. L., Oppenheimer, N., Garvy, B., Kusser, K., Goodrich, S., Howard, M., Harmsen, A., Randall, T. D., and Lund, F. E. (2001) Cyclic ADP-ribose production by CD38 regulates intracellular calcium release, extracellular calcium influx and chemotaxis in neutrophils and is required for bacterial clearance in vivo. *Nat. Med.* **7,** 1209–1216
23. Galione, A., and Petersen, O. H. (2005) The NAADP Receptor: New Receptors or New Regulation? *Mol. Interv.* **5,** 73–79
24. Santella, L. (2005) NAADP: A New Second Messenger Comes of Age. *Mol. Interv.* **5,** 70–72
25. Lee, H. C. (2004) Multiplicity of Ca^{2+} messengers and Ca^{2+} stores: a perspective from cyclic ADP-ribose and NAADP. *Curr. Mol. Med.* **4,** 227–237
26. Langhorst, M. F., Schwarzmann, N., and Guse, A. H. (2004) Ca^{2+} release via ryanodine receptors and Ca^{2+} entry: major mechanisms in NAADP-mediated Ca^{2+} signaling in T-lymphocytes. *Cell Signal* **16,** 1283–1289
27. Yamasaki, M., Thomas, J. M., Churchill, G. C., Garnham, C., Lewis, A. M., Cancela, J. M., Patel, S., and Galione, A. (2005) Role of NAADP and cADPR in the induction and maintenance of agonist-evoked Ca^{2+} spiking in mouse pancreatic acinar cells. *Curr. Biol.* **15,** 874–878
28. Wilding, M., Russo, G. L., Galione, A., Marino, M., and Dale, B. (1998) ADP-ribose gates the fertilization channel in ascidian oocytes. *Am. J. Physiol.* **275,** C1277–1283
29. Billington, R. A., Ho, A., and Genazzani, A. A. (2002) Nicotinic acid adenine dinucleotide phosphate (NAADP) is present at micromolar concentrations in sea urchin spermatozoa. *J. Physiol.* **544,** 107–112
30. Turner, H., Fleig, A., Stokes, A., Kinet, J. P., and Penner, R. (2003) Discrimination of intracellular calcium store subcompartments using TRPV1 (transient receptor potential channel, vanilloid subfamily member 1) release channel activity. *Biochem. J.* **371,** 341–350

Received for publication November 28, 2005.
Accepted for publication December 28, 2005.